LANGMUIR
Cite This: *Langmuir* 2018, 34, 12244−12250
Article
pubs.acs.org/Langmuir

Extraction of Silicone Uncrosslinked Chains at Air−Water−Polydimethylsiloxane Triple Lines

Aurélie Hourlier-Fargette,*[,†,‡] Julien Dervaux,[§] Arnaud Antkowiak,[†,∥] and Sébastien Neukirch[†]

[†]Sorbonne Université, Centre National de la Recherche Scientifique, UMR 7190, Institut Jean Le Rond d'Alembert, F-75005 Paris, France

[‡]Département de Physique, École Normale Supérieure, CNRS, PSL Research University, F-75005 Paris, France

[§]Matière et Systèmes Complexes, CNRS UMR 7057, Université Paris Diderot, Sorbonne Paris Cité University, F-75013 Paris, France

[∥]Surface du Verre et Interfaces, UMR 125 CNRS/Saint-Gobain, F-93303 Aubervilliers, France

Supporting Information

ABSTRACT: Silicone elastomers such as polydimethylsiloxane (PDMS) are convenient materials routinely used in laboratories that combine ease of preparation, flexibility, transparency, and gas permeability. However, these elastomers are known to contain a small fraction of uncrosslinked low-molecular-weight oligomers, the effects of which are not completely understood, particularly when used in contact with liquids. Here, we show that triple lines involving air, water, and PDMS elastomers are responsible for the contamination of water−air interfaces by uncrosslinked silicone oligomers through a capillarity-induced extraction mechanism. We investigate both the case of static and moving contact lines and study various geometries ranging from partially immersed PDMS plates to water droplets or air bubbles deposited on PDMS plates, all involving air−water−elastomer triple lines. We demonstrate experimentally that the contamination timescale is strikingly shorter for moving contact lines than in the static case. Eventually, we propose a simple poroelastic model capturing the main features of contamination observed in experiments.

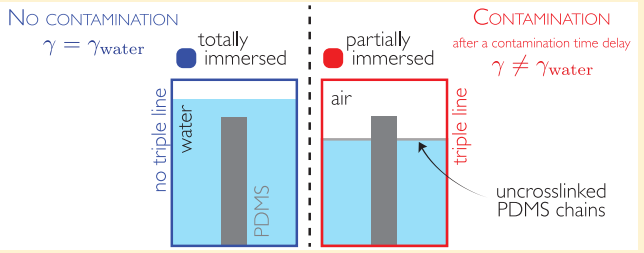

INTRODUCTION

The understanding of interactions between silicone elastomers or gels and aqueous liquids is of crucial interest in all situations where these two ingredients come into play, from elastocapillarity experiments[1] to lab-on-a-chip studies,[2] with applications in physics, chemistry, biology, materials science, and bioengineering. Among silicone elastomers, polydimethylsiloxane (PDMS) is a popular and easy-to-use material for rapid prototyping, as it is patternable by soft lithography, optically transparent, gas-permeable, and flexible.[3] This material is thus a good candidate to build microchannels for numerous applications such as vesicles or bubbles production and manipulation,[4] cell cultures and organs-on-a-chip,[5] or biomedical diagnostics.[6] Silicone elastomers have nevertheless some drawbacks as follows: leaching of uncrosslinked oligomers from the polymer network into microchannel media has been reported in the context of cell culture in PDMS devices.[7,8] Commercial silicone elastomers such as Dow Corning SYLGARD 184 PDMS indeed consist of a cross-linked polymer network but also contain a small fraction of silicone uncrosslinked chains that are not incorporated into the network during the cross-linking process.[9] Beyond the recent interest for capillarity on soft solids,[10,11] a better awareness of potential interactions between liquids and silicone elastomers related to capillary effects is essential to avoid or control contamination of liquid interfaces by uncrosslinked oligomers.

Consequences of the presence of uncrosslinked chains in silicone elastomers have been recently investigated in the context of adhesion,[12] osmocapillary phase-separation,[13] superhydrophobic drag reduction,[14] swelling of composite structures,[15] and droplet dynamics,[16] revealing that the existence of uncrosslinked chains at the scale of the polymer network can lead to significant macroscopic effects. When a silica microbead is deposited on a PDMS gel, adhesion leads to a phase separation;[12] some liquid PDMS is extracted from the core of the gel at the contact line, replacing the usual three-phase contact line by a four-phase contact zone with air, silica, liquid PDMS, and gel PDMS. The question of the extraction of uncrosslinked chains is also raised when a small cavity exists at the surface of a gel, involving a competition between osmosis and capillarity.[13] Additionally, traces of surfactants, possibly due to PDMS uncrosslinked chains, have been shown to severely limit the drag reduction of superhydrophobic surfaces.[14] Although the presence of uncrosslinked chains is

Received: June 22, 2018
Revised: August 29, 2018
Published: September 10, 2018

DOI: 10.1021/acs.langmuir.8b02128
Langmuir 2018, 34, 12244−12250

often seen as a drawback, taking advantage of uncrosslinked oligomers in silicone elastomers may also lead to functionality, shaping composite structures to form three-dimensional structures from two-dimensional patterns via residual swelling.[15]

In a previous work,[16] we have shown that a water (or water−glycerol mixture) droplet deposited on an inclined plane made of a silicone elastomer that contains uncrosslinked chains exhibits unusual dynamics, with two successive speed regimes, as shown in Figure 1a. This result could not be explained by

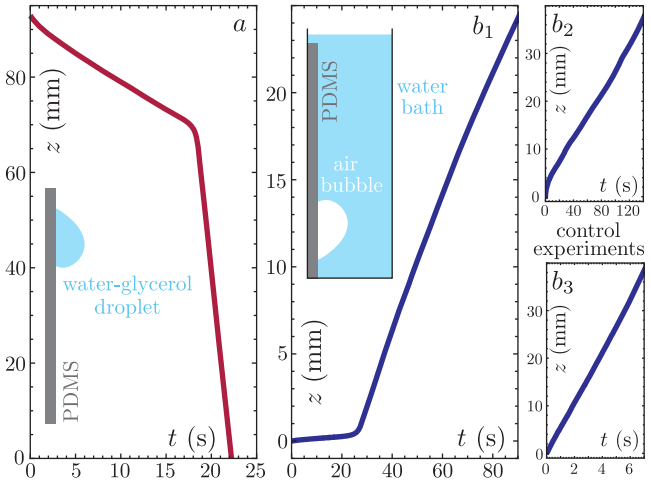

Figure 1. (a) A droplet (40% water−60% glycerol mixture) of volume 21.5 μL is deposited on a vertical PDMS plate. Its height is recorded as a function of time, and two successive speed regimes are identified. (b) A setup where phases are reversed is investigated: (b_1) an air bubble is deposited on a vertical PDMS plate immersed in a water bath, and its height is recorded as a function of time. Two successive speed regimes are also identified. (b_2,b_3) As control experiments, similar air bubbles are deposited on toluene-washed PDMS (from which uncrosslinked chains have been extracted with toluene prior to the experiment) (b_2) and on a thin polyester film (b_3); in both cases, bubbles exhibit a single speed regime.

mechanisms previously reported on droplet dynamics on solid substrates.[17,18] The existence of the second speed regime of a droplet on a silicone elastomer was directly linked to the presence of uncrosslinked chains in the elastomer as (i) the unusual behavior disappeared when treating the elastomer to remove the uncrosslinked chains and (ii) an oil film was clearly visible at the surface of a beaker in which thousands of droplets were collected. Nevertheless, the exact process by which contamination of the drop surface takes place, its speed, and locus remained unclear. Moreover, an alternative continuous indicator (apart from the sliding speed) of whether or not a drop is contaminated by uncrosslinked oil chains was missing.

Here, we show that contact lines, whether static or in motion, mediate the contamination of droplets, and we propose that this contamination is promoted by a poroelastic capillarity-induced extraction of oligomers at the contact line. We first demonstrate that the extraction of uncrosslinked chains observed in the case of a droplet moving on a silicone elastomer inclined plane[16] also exists in various situations where sessile or moving air−water−silicone elastomer contact lines are present (e.g., air bubbles rising up on an immersed PDMS inclined plane). Studies of oil thin films on water baths have been performed more than one century ago for natural oils[19−21] and more recently for PDMS oils,[22] showing that surface tension sharply decreases once a critical surface concentration of oil chains is reached. Building on tensiometry and ellipsometry results from Lee et al.,[22] we conjecture that the sharp transition in the speed of droplets and bubbles is linked to the transition from patches of PDMS to a complete layer of PDMS on the water−air interface, the transition occurring once a critical surface concentration in uncrosslinked chains is reached. By performing surface tension measurements on a single droplet stopped at various positions during its descent, we indeed demonstrate that the transition in speed occurs exactly at the same time as the transition in surface tension. Depending on the situation observed (moving or sessile interfaces), either of the two parameters (speed and surface tension) is then used to quantify contamination of the water−air interface. We further establish the critical role of the presence of a water−air−PDMS contact line by comparing two simple situations: a PDMS sample completely immersed in water and a PDMS sample partially immersed in water. We evidence that the two setups lead to completely different results in terms of contamination of water−air interfaces, showing that contamination is mainly mediated by the contact line. We then study quantitatively the timescales involved in contamination of water−air interfaces in the case of sessile and moving water−air−PDMS contact lines. Eventually, we put forward an elementary model explaining contamination as a poroelastic oligomer extraction process driven by capillarity, recovering the salient features of contamination observed experimentally.

EXPERIMENTAL METHODS

Elastomers. The elastomer samples were made of PDMS (Dow Corning SYLGARD 184 elastomer base blended with its curing agent in proportion 10:1 by weight, cured during 2 h at 60 °C) molded in 12 cm × 12 cm Petri dishes to obtain flat samples with a thickness of a few millimeters. The surface used in all droplet deposition experiments was the top surface, cured in contact with air. The Young's modulus of our PDMS samples, measured with a Shimadzu testing machine, was found to be $E = 1.8 \pm 0.1$ MPa.

Extraction of Uncrosslinked Chains. Control experiments involve PDMS samples treated with toluene to remove uncrosslinked chains.[16] The extraction procedure was the following: (i) samples were immersed in toluene (with no continuous agitation) for 1 week, the toluene bath being changed everyday to avoid saturation in uncrosslinked chains, (ii) samples were then deswollen by progressively replacing toluene by a poor solvent of PDMS, namely, ethanol, and (iii) samples were dried out in a vacuum oven. Contact angles on toluene-treated samples are similar to nontreated samples (a difference in advancing and receding angles of less than 10° was noticed between treated and nontreated samples).

Liquids. Droplets of deionized water (of volume comprised between 5 and 75 μL) were deposited on polymer samples with an electronic micropipette (Sartorius eLINE 5−120 μL), with the lowest deposition speed available.

Rapid Imaging Acquisition and Analysis. Videos have been captured with a Hamamatsu Orca Flash digital CMOS camera, with frame rates going from 10 to 1000 frames per second. Image analysis has been performed with ImageJ software.

Surface Tension Measurements. To record surface tension as a function of time or to measure surface tension of a single droplet, Kibron EZ-Pi+ or MTX tensiometers were used with a 500 μm diameter cylindrical platinum probe, cleaned before each measurement with a butane torch. Measuring surface tension of a small droplet with this probe however requires to take into account the Laplace pressure due to the curvature of the interface; the difference between surface tension measured in the case of a droplet and the surface tension of a flat bath of the same liquid evolves as a function of

DOI: 10.1021/acs.langmuir.8b02128
Langmuir 2018, 34, 12244−12250

the radius of curvature of the drop, as explained in the Supporting Information and shown in Figure S1.

RESULTS AND DISCUSSION

Contamination at Triple Lines. *Moving Droplets and Bubbles.* A water—or water−glycerol mixture—droplet sliding down on a vertical PDMS plate exhibits two successive speed regimes because of contamination of the water−air interface of the droplet by silicone uncrosslinked chains.[16] A typical height versus time diagram is shown in Figure 1a. Even though the droplet might be progressively covered by uncrosslinked chains, the change to the second speed regime is abrupt. On the basis of measurements from Lee et al.,[22] we postulate that the second regime is attained once a complete layer of uncrosslinked chains is reached on the droplet.

We now focus on what happens when reversing the phases, namely, looking at an air bubble rising up an immersed PDMS plate. We first consider the case of a bubble sliding up a vertical solid plate with no uncrosslinked chains. The question of the final speed of such a bubble is mathematically identical to the question of the final speed of a droplet sliding down a vertical plate,[23] except that in the bubble setup, dissipation in the fluid phases mainly occurs in the surrounding liquid and not in the moving object. The simplest approach predicts that an air bubble should reach a final constant speed after a short transient. We check this hypothesis experimentally by carrying out two control experiments on a PDMS plate treated with toluene to remove its uncrosslinked chains (Figure 1b$_2$) and on a vertical polyester plate that does not contain uncrosslinked chains (Figure 1b$_3$). In both cases, we find that the air bubble exhibits a single sliding regime. Now turning to bubble dynamics on a PDMS plate with uncrosslinked chains, we find two sliding regimes, as shown in Figure 1b$_1$.

This result suggests that the contamination of the water−air interface is linked to the presence of a water−air−PDMS contact line rather than to the existence of a rolling motion inside the droplet, as the liquid flows are different in the bubble case than in the droplet case. To further investigate contamination at both moving and sessile contact lines, we then focus on the link between the speed transition and the properties of the liquid−air interface.

Relationship between Speed and Surface Tension. As shown by Hourlier-Fargette et al.,[16] the surface tension of a sliding droplet varies between the beginning and the end of its two-regime descent on a PDMS sample. Here, to be able to record the surface tension of a droplet during its descent, we design the following experiment: a deionized water droplet of volume V = 45 μL is deposited on a Dow Corning SYLGARD 184 PDMS inclined plane, making an angle equal to 45° with the horizontal. Once the droplet has traveled a distance d on the inclined plane, the plane is moved back into a horizontal position, and the surface tension of the droplet is measured as a function of d with a Kibron EZ-Pi+ tensiometer. To induce minimal disruption in the system, a new droplet is used for each d value studied. Therefore, each droplet travels a distance d before its surface tension is measured within 30 s, and then, the droplet is thrown away. The 45° tilting angle is chosen to make the tilting step easier. The volume of the droplet is also chosen for its speed to be small enough to allow us to move the plane back to a horizontal position in a time lapse during which the distance traveled by the droplet is negligible compared to d.

Measurements of surface tension as a function of the distance d traveled by the droplet are shown in Figure 2b,

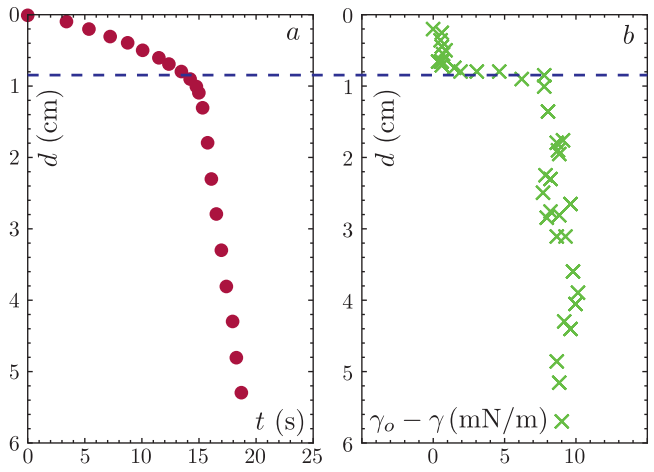

Figure 2. (a) Distance versus time diagram: d is the distance traveled by the droplet and t is time. (b) Distance versus surface tension diagram, $\gamma_o - \gamma$ is the difference between the surface tension γ_o of pure water and the actual surface tension γ of a droplet that has traveled a distance d. The water droplets have volume V = 45 μL and are deposited on a 45° inclined plane made of Dow Corning SYLGARD 184 PDMS. Speed transition coincides with surface tension transition; during the first regime, the droplet has a surface tension equal to the surface tension of pure water, whereas during the second regime, its surface tension takes on another, lower, surface tension value.

where a sharp transition is observed once the droplet has traveled 8 mm. For comparison we also show in Figure 2a the distance versus time diagram for the same setup, namely, a 45 μL water droplet on a 45° PDMS tilted plane. These results demonstrate that the speed transition occurs at the same time as a sudden surface tension transition from a value equal to the surface tension of pure water to a lower, constant, value. More precisely, we show experimentally that both transitions occur at a same distance and hence at the same time. The transition time between the two regimes can thus be identified in two different ways as follows: by looking at the speed of a droplet or by measuring its surface tension.

Sessile Droplets. We now consider contamination of water−air interfaces in the case of sessile contact lines, and we use surface tension as a parameter to quantify the evolution of the contamination of the droplet as a function of time. The experiments performed in the previous section establish that quantifying the contamination timescale can be done in an equivalent manner by using either of the two parameters studied, namely, speed and surface tension. Figure 3 shows the surface tension of a sessile droplet as a function of time. A sharp decrease is observed after a few minutes. This sharp transition is used to define the contamination time τ_c as the time for which the surface tension takes a mean value between its initial and final values. Contamination timescales for sessile droplets are much larger than contamination timescales observed for moving droplets and are investigated further in the section entitled Contamination Timescales, which includes the study of the influence of droplet size on contamination timescales, as well as a simple poroelastic modeling of those experimental results.

DOI: 10.1021/acs.langmuir.8b02128
Langmuir 2018, 34, 12244−12250

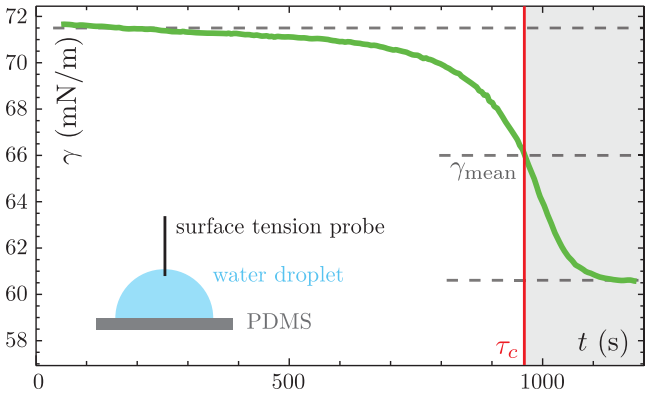

Figure 3. A deionized water droplet (15 μL) is deposited on a horizontal Dow Corning SYLGARD 184 PDMS plate. Its surface tension is recorded as a function of time, and a neat fall-off in surface tension is observed at a time that is later referred to as τ_c (contamination time). More precisely, τ_c is defined as the time at which the average value of the initial and final surface tension, γ_{mean}, is reached. We conjecture, building on Lee et al.,[22] that after τ_c (light gray zone on the graph), a complete layer of uncrosslinked chains is formed on the droplet.

Role of the Triple Line. To give evidence of the crucial role of the triple line in contamination, we compare two situations where PDMS is in contact with water, with the first setup involving a water−air−PDMS contact line and the second one being free of any contact line. We use two Petri dishes with diameter 5.5 cm. In each Petri dish, we lay out five PDMS columns, two with dimensions 4 cm × 0.8 cm × 0.5 cm and three with dimensions 2 cm × 0.8 cm × 0.5 cm.

In the first Petri dish, the water level is chosen to be smaller than the height of the PDMS columns (partially immersed situation, shown in red in Figure 4), whereas in the second Petri dish, the water level is a few millimeters larger than the height of the PDMS columns (totally immersed situation, shown in blue in Figure 4). We record the surface tension of

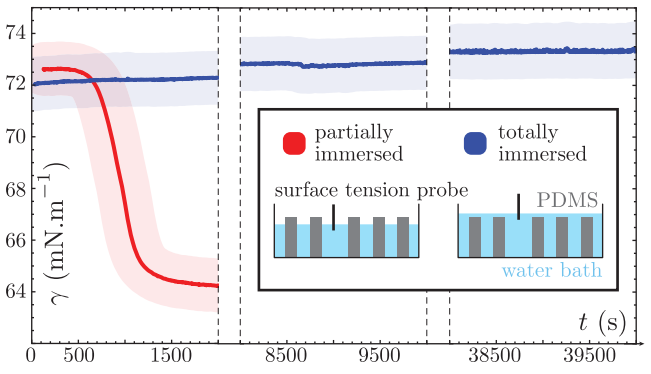

Figure 4. Surface tension of a water bath is recorded as a function of time in two situations; the first Petri dish contains partially immersed PDMS plates (red), whereas the second Petri dish contains completely immersed PDMS plates (blue). We observe a sharp surface tension transition for the partially immersed situation, whereas surface tension in the totally immersed situation stays stable during the whole recording time (the small increase of the measured surface tension observed in the blue curve is due to the change in water level due to evaporation; the probe was immersed deeper than usual to avoid detachment from the liquid bath after a long recording time and was thus subjected to Archimede's pressure). The uncertainties on the measurements are represented on the large pale colors stripes.

the water interface at the surface of both Petri dishes and observe that in the case of partially immersed plates, a sharp decrease occurs around 15 min. In the case of totally immersed plates, we have not noticed any significant modification of the surface tension in more than 10 h. This experiment gives evidence that extraction is driven by the presence of a contact line.

We further investigate the critical role of the contact line in contamination of the water−air interface by varying the immersion depth of PDMS plates with constant water−air−PDMS contact line contour length. Two Dow Corning SYLGARD 184 PDMS plates are partially immersed in a water bath, as shown in Figure 5, with two different immersion

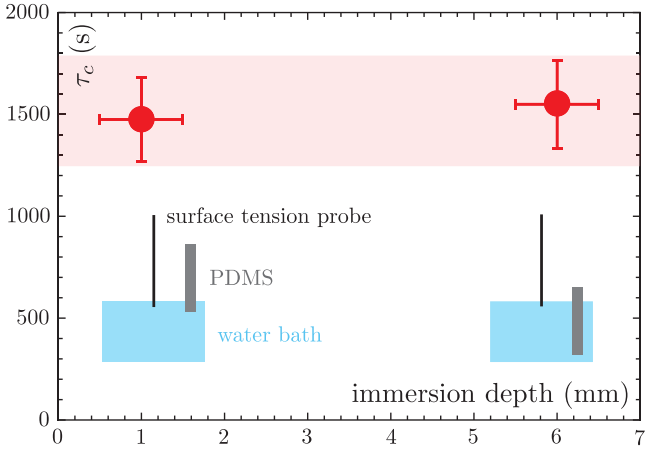

Figure 5. Dependence of the contamination time τ_c as function of the immersion depth. Dow Corning SYLGARD 184 plates are partially immersed in a water bath of total area 4 cm^2. The perimeter of the contact line between PDMS and water is 36 mm. Each point on the graph is an average of four identical measurements, and the error bars correspond to statistical uncertainties. An increase of the immersion depth by more than a factor 5 leads to no significant modification of the contamination time τ_c. The light red band is a guide for the eye and illustrates that, given the uncertainties, the contamination times in the two cases can be considered to be equal.

depths. The total area of PDMS in contact with water is multiplied by a factor larger than 5 between the two setups; if a significant amount of PDMS chains are extracted at other locations than the triple line, the contamination time should be significantly different in the two setups. For each immersion depth, four identical experiments are performed. The results, displayed in Figure 5, correspond to the average of the measurements for each immersion depth, error bars being representative of the statistical uncertainties. No significant difference is observed in the contamination time τ_c between the two setups, giving additional evidence that extraction of uncrosslinked chains essentially occurs at the triple line.

Contamination Timescales. *Sessile Droplets.* We now focus on contamination timescales and investigate first the contamination dynamics of a sessile droplet as a function of the droplet size. Our experimental setup is the following: a droplet of volume V is deposited on a horizontal Dow Corning SYLGARD 184 PDMS plate, and its surface tension is recorded as a function of time. The contamination time τ_c is determined for each droplet volume by taking the average of one to three measurements, and the error bars are representative of statistical uncertainties. Volumes ranging from 5 to 75 μL are investigated. The contamination time τ_c is

DOI: 10.1021/acs.langmuir.8b02128
Langmuir 2018, 34, 12244−12250

then plotted in Figure 6 as a function of the base radius of the droplet R, calculated from the droplet volume V by assuming

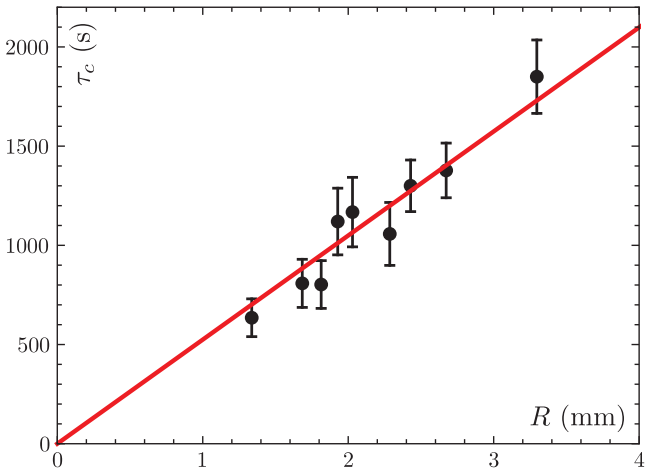

Figure 6. Contamination time τ_c as a function of the base radius R of a sessile water droplet deposited on a Dow Corning SYLGARD 184 plate. Each point is an average of one to three measurements, the error bars being representative of statistical uncertainties. The red line is a linear fit, showing that our results are compatible with a linear relation $\tau_c \propto R$.

that the droplet is a half sphere. A first conclusion is that the timescales recorded for sessile droplet contamination are much longer than typical timescales involved in the case of moving droplets or bubbles. We also observe that the experimental results exhibit a rather linear relationship between the contamination time τ_c and the base radius R, a relationship that will be analyzed further in the next section.

Moving Droplets. Contamination of moving droplets involves much shorter timescales than sessile droplets. However, at a fixed droplet size, the contamination timescale—defined as the time at which the second speed regime is reached—depends on the speed of the droplet. To quantify the evolution of the contamination timescale as a function of the droplet speed, our experimental setup is the following: water droplets of constant volume are deposited on PDMS inclined planes, and the angle of inclination is varied to change the droplet speed in the first regime without affecting its volume. Changing the inclination angle instead of the droplet volume allows us to reach different speeds without varying significantly the perimeter of the contact line (which is a parameter that is likely to influence the contamination time given results obtained for sessile droplets). Experiments are performed with three droplet volumes to rapidly test the influence of the droplet size. The contamination time is recorded as a function of the speed of the droplet and shown in a log−log diagram in Figure 7. The yellow triangles correspond to 20 μL droplets, orange dots correspond to 40 μL droplets, and red squares correspond to 60 μL droplets. The angles of inclination are varied between 57° and 90° for 20 μL droplets, between 33° and 45° for 40 μL droplets, and between 24° and 35° for 60 μL droplets. The droplet shapes are slightly different when changing the angle of the inclined plane, but to first order, this shape modification will be neglected in the discussion. No significant difference is observed between the curves for the different volumes. This can be explained by the limited volume variation range accessible in our experiments; droplets of smaller volumes are immobile on a vertical plane because of pinning forces, whereas droplets of larger volume form puddles. Uncertainties, which are mainly statistical and can be estimated through the scatter of our data, do not allow us to distinguish between the three volume cases. A power law with a negative exponent (lower than unity in absolute value, close to −2/3) fits the data well, except from a small deviation at small speeds. This deviation was to be expected, as the contamination time in the case of a sessile droplet is not infinite. Further analysis of the experimental scaling law established here is performed in the following section.

Contamination Timescales: A Scaling Approach. In a poroelastic material, solvent molecules (free chains in the case of PDMS) move in response to gradients of chemical potential (also known as the "pore pressure"), which depends on both the local solvent concentration and the state of stress of the material.[24] At the triple line between an elastic solid, a vapor phase, and a liquid phase, capillarity leads to the formation of a sharp ridge beneath the contact line where the elastic material is under tension.[25,26] The characteristic length of this ridge is given by the elastocapillary length[27] $l_s \approx \gamma_s/E$, where γ_s and E are, respectively, the surface tension and the elastic modulus of PDMS. As theoretically suggested recently,[27] this tension may induce the migration of free chains and their accumulation

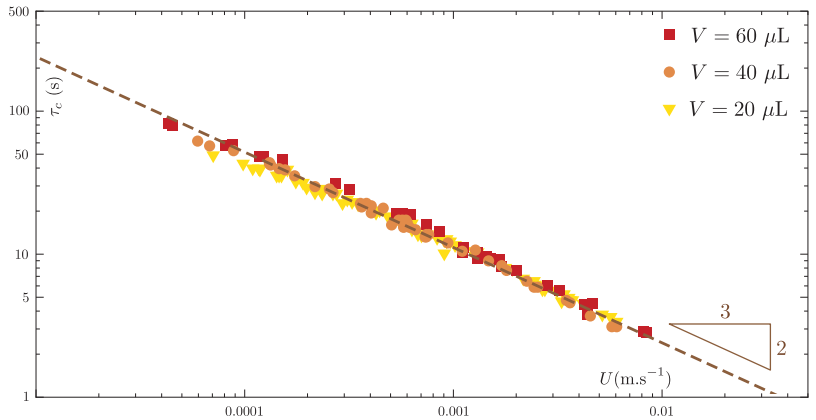

Figure 7. Water droplets of volumes 20 μL (yellow triangles), 40 μL (orange dots), and 60 μL (red squares) are deposited on Dow Corning SYLGARD 184 PDMS inclined planes. The angle of inclination is varied to change the droplet speed. We record the contamination time τ_c as a function of the droplet speed in the first regime U and show that our data are consistent with a −2/3 power law scaling (brown dashed line).

DOI: 10.1021/acs.langmuir.8b02128
Langmuir 2018, 34, 12244−12250

within the ridge. This diffusive process occurs on a typical timescale $t_{diff} = l_s^2/D$, where D is the effective diffusion coefficient of the free chains in the cross-linked network, estimated to be in the range 10^{-12} to 10^{-11} m^2/s.[27,28] In our system, l_s is around 10 nm, and the timescale t_{diff} is thus of the order of 10 to 100 μs. Because it is energetically favorable for PDMS chains to cover the surface of the water droplet, there is a flux of chains per unit area J from the concentrated ridge toward the surface of the drop.

At small times ($t \ll t_{diff}$), this flux diverges as $\sim 1/\sqrt{t}$, whereas at $t \to \infty$, it vanishes as the chemical potentials of the PDMS chains in the elastomer and at the surface of the drop will be equal.[29] However, if we assume that the diffusion of the chains at the surface of the drop is significantly faster[30] than their diffusion throughout the elastomer/droplet interface, then while the concentration of chains is much higher in the PDMS ridge (which acts as an infinite reservoir of free chains) than at the surface of the drop, the flux J will be constant and essentially proportional to the free chain concentration in the elastomer. We assume that the diffusive process of the chains through the triple line is the limiting process and will check the consistency of this hypothesis shortly thereafter.

Model for Sessile Droplets. The total flux J_{tot} of small molecules from the PDMS ridge toward the surface of the drop can be estimated as the flux J multiplied by an area. As mentioned previously, uncrosslinked chains are essentially concentrated in the elastocapillary ridge which, in three dimensions, is a ring of length proportional to R and of thickness l_s. The total flux from PDMS to the drop surface is therefore simply given by $J_{tot} \approx JRl_s$ and thus behaves as $J_{tot,small\ t} \propto Rl_s/\sqrt{t}$ at small times and as $J_{tot,large\ t} \propto Rl_s$ at large times. Now, the total number of free chains $N(t)$ at the free surface of the drop at time t is given by the integral $N(t) = \int_0^t J_{tot}(t)dt$. Furthermore, there exists a critical number N_c of free chains at the free surface of the drop that triggers the surface tension transition. This number is proportional to the area of the drop, $N_c \propto \rho_c R^2$, where ρ_c is the critical surface concentration of free chains. As a consequence, the transition occurs at the critical time τ_c when the total number of extracted molecules $N(\tau_c)$ reaches the critical number N_c that is

$$N(\tau_c) = \int_0^{\tau_c} J_{tot}\, dt = N_c \propto \rho_c R^2 \tag{1}$$

For large sessile drops, the timescale of contamination is much longer than the diffusive timescale t_{diff}. In this limit, the relevant flux of free chains from the solid to the droplet is thus the large time flux $J_{tot,large\ t} \propto Rl_s$. Inserting this expression in the equation above, one obtains a critical contamination time

$$\tau_{c,sessile\ drop} \propto \frac{\rho_c R}{l_s} \tag{2}$$

showing that the contamination time is indeed proportional to the base radius R of the drop and thus in good agreement with the results of Figure 6.

Model for Moving Droplets. If now the drop is in motion, the typical width of the ring acting as a reservoir of uncrosslinked chains is no longer the elastocapillary length l_s but the length scanned during the motion of the drop Ut where U is the velocity of the drop. The total flux from the solid to the drop surface is simply $J_{tot} \propto JRUt$ and thus behaves as $J_{tot,small\ t} \propto RUt/\sqrt{t}$ at small times and as $J_{tot,large\ t} \propto RUt$ at large times. If the drop moves fast enough (i.e., $U \gg l_s/t_{diff} \approx 10^{-4}$ m/s), as it is the case in our experimental setup, the relevant approximation for the flux of uncrosslinked chains is thus $J_{tot,small\ t} \propto RUt/\sqrt{t}$. Inserting this expression in eq 1 leads to the critical contamination time

$$\tau_{c,moving\ drop} \propto \left(\frac{\rho_c R}{U}\right)^{2/3} \tag{3}$$

where we recover the scaling $U^{-2/3}$ observed in the experiments shown in Figure 7. As $U \to 0$, the critical time τ_c is not diverging, as observed in Figure 6. Consequently, the scaling $U^{-2/3}$ is eventually lost at small speeds for which we expect a quantitatively different behavior, with a weaker influence of the velocity on the contamination time. Hence, the present simple model is unlikely to predict contamination timescales at low to intermediate velocities because it would be necessary to take into account the full time-dependent evolution of the concentration field in the ridge, which is outside the scope of this study.

In addition, we estimate the diffusion coefficient of the PDMS chains across the triple line. From the slope of the curve $\tau_c(R)$ shown in Figure 6, as well as an estimation of the critical surface concentration, $\rho_c \approx 0.7$ mg/m^2,[22] we evaluate the linear mass flow rate from PDMS to the drop as $Q = \rho_c R/\tau_c \approx 10^{-6}$ mg/m/s. As mentioned previously, we have assumed that this rate is directly proportional to the concentration of free chains in the ridge. Although this concentration is not known, we may broadly estimate its value to lie between the typical concentration of free chains in a PDMS elastomer ($\sim$5%[9,16]) and that of a fully liquified ridge (100%). Because the volumetric mass density of PDMS is around 1000 kg/m^3, the diffusion coefficient of the chains across the interface is therefore in the range $Q/\rho \approx 10^{-15}$ to 10^{-13} m^2/s. This value is well below the diffusion coefficient of PDMS chains within the cross-linked network[27] and thus consistent with our earlier hypothesis that the limiting process for the droplet contamination is the crossing of the elastomer surface by the PDMS chains.

CONCLUSIONS

We have shown that silicone uncrosslinked chains present in most commonly used silicone elastomers contaminate air−water interfaces when an air−water−silicone elastomer contact line is present. By performing experiments in several configurations, with droplets, bubbles, and water baths, we have demonstrated that the contact line does not need to move to promote interfacial contamination; modifications of the air−water interfacial properties have been highlighted both in the case of moving and sessile contact lines. Contamination timescales have been shown to differ from several orders of magnitude between sessile and moving contact lines. More precisely, the migration of silicone uncrosslinked chains to the interface leads to a sharp surface tension transition once a critical surface concentration in chains is reached. This transition is defined as the contamination timescale. In the context of moving contact lines, we have found that the surface tension transition occurs exactly at the moment when a sharp speed transition is observed, which makes this transition visually striking. For sessile contact lines, surface tension was

DOI: 10.1021/acs.langmuir.8b02128
Langmuir 2018, 34, 12244−12250

recorded to determine the contamination timescale. The use of those two physical parameters allowed us to collect measurements both for sessile and moving contact lines, which have been successfully compared to a simple model using a diffusion-driven mechanism for the migration of the chains.

Soft materials and especially silicone elastomers are widely used in contact with water in many research fields. However, interactions between silicone elastomers and liquids are often forgotten but can lead to unexpected behaviors that can be explained in the light of the present work.

■ ASSOCIATED CONTENT

Supporting Information

The Supporting Information is available free of charge on the ACS Publications website at DOI: 10.1021/acs.langmuir.8b02128.

Experimental technique used to measure the surface tension of a single droplet, taking into account the Laplace pressure and showing the normalized difference between the measured surface tension for a droplet and the surface tension of an infinite liquid bath (PDF)

■ AUTHOR INFORMATION

Corresponding Author

*E-mail: aurelie.fargette@dalembert.upmc.fr.

ORCID

Aurélie Hourlier-Fargette: 0000-0002-0148-4145

Notes

The authors declare no competing financial interest.

■ ACKNOWLEDGMENTS

We thank Emmanuelle Rio and Vivek Sharma for their support in the experiments involving Kibron tensiometers, Antoine Chateauminois for his help in the preparation of toluene-washed elastomer samples for control experiments, and Paul Grandgeorge for enlightening discussions. The present work was supported by ANR grant ANR-14-CE07-0023-01.

■ REFERENCES

(1) Bico, J.; Reyssat, É.; Roman, B. Elastocapillarity: When Surface Tension Deforms Elastic Solids. *Annu. Rev. Fluid Mech.* **2018**, *50*, 629−659.

(2) Whitesides, G. M. The origins and the future of microfluidics. *Nature* **2006**, *442*, 368−373.

(3) Mukhopadhyay, R. When PDMS isn't the best. *Anal. Chem.* **2007**, *79*, 3248−3253.

(4) Gañán Calvo, A. M.; Gordillo, J. M. Perfectly Monodisperse Microbubbling by Capillary Flow Focusing. *Phys. Rev. Lett.* **2001**, *87*, 274501.

(5) Huh, D.; Torisawa, Y.-s.; Hamilton, G. A.; Kim, H. J.; Ingber, D. E. Microengineered physiological biomimicry: Organs-on-Chips. *Lab Chip* **2012**, *12*, 2156−2164.

(6) Chin, C. D.; et al. Microfluidics-based diagnostics of infectious diseases in the developing world. *Nat. Med.* **2011**, *17*, 1015−1019.

(7) Berthier, E.; Young, E. W. K.; Beebe, D. Engineers are from PDMS-land, Biologists are from Polystyrenia. *Lab Chip* **2012**, *12*, 1224−1237.

(8) Regehr, K. J.; Domenech, M.; Koepsel, J. T.; Carver, K. C.; Ellison-Zelski, S. J.; Murphy, W. L.; Schuler, L. A.; Alarid, E. T.; Beebe, D. J. Biological implications of polydimethylsiloxane-based microfluidic cell culture. *Lab Chip* **2009**, *9*, 2132−2139.

(9) Lee, J. N.; Park, C.; Whitesides, G. M. Solvent Compatibility of Poly(dimethylsiloxane)-Based Microfluidic Devices. *Anal. Chem.* **2003**, *75*, 6544−6554.

(10) Andreotti, B.; Bäumchen, O.; Boulogne, F.; Daniels, K. E.; Dufresne, E. R.; Perrin, H.; Salez, T.; Snoeijer, J. H.; Style, R. W. Solid capillarity: when and how does surface tension deform soft solids? *Soft Matter* **2016**, *12*, 2993−2996.

(11) Style, R. W.; Jagota, A.; Hui, C.-Y.; Dufresne, E. R. Elastocapillarity: Surface Tension and the Mechanics of Soft Solids. *Annu. Rev. Condens. Matter Phys.* **2017**, *8*, 99−118.

(12) Jensen, K. E.; Sarfati, R.; Style, R. W.; Boltyanskiy, R.; Chakrabarti, A.; Chaudhury, M. K.; Dufresne, E. R. Wetting and phase separation in soft adhesion. *Proc. Natl. Acad. Sci. U.S.A.* **2015**, *112*, 14490−14494.

(13) Liu, Q.; Suo, Z. Osmocapillary phase separation. *Extreme Mech. Lett.* **2016**, *7*, 27−33.

(14) Peaudecerf, F. J.; Landel, J. R.; Goldstein, R. E.; Luzzatto-Fegiz, P. Traces of surfactants can severely limit the drag reduction of superhydrophobic surfaces. *Proc. Natl. Acad. Sci. U.S.A.* **2017**, *114*, 7254−7259.

(15) Pezzulla, M.; Shillig, S. A.; Nardinocchi, P.; Holmes, D. P. Morphing of geometric composites via residual swelling. *Soft Matter* **2015**, *11*, 5812−5820.

(16) Hourlier-Fargette, A.; Antkowiak, A.; Chateauminois, A.; Neukirch, S. Role of uncrosslinked chains in droplets dynamics on silicone elastomers. *Soft Matter* **2017**, *13*, 3484−3491.

(17) Le Grand, N.; Daerr, A.; Limat, L. Shape and motion of drops sliding down an inclined plane. *J. Fluid Mech.* **2005**, *541*, 293−315.

(18) Puthenveettil, B. A.; Senthilkumar, V. K.; Hopfinger, E. J. Motion of drops on inclined surfaces in the inertial regime. *J. Fluid Mech.* **2013**, *726*, 26−61.

(19) Pockels, A. On the Relative Contamination of the Water-Surface by Equal Quantities of Different Substances. *Nature* **1892**, *46*, 418−419.

(20) Rayleigh, L. XXXVI. Investigations in Capillarity:-The size of drops.-The liberation of gas from supersaturated solutions.-Colliding jets.-The tension of contaminated water-surfaces. *London, Edinburgh Dublin Philos. Mag. J. Sci. 5* **1899**, *48*, 321−337.

(21) Langmuir, I. The constitution and fundamental properties of solids and liquids. II. Liquids. *J. Am. Chem. Soc.* **1917**, *39*, 1848−1906.

(22) Lee, L. T.; Mann, E. K.; Langevin, D.; Farnoux, B. Neutron reflectivity and ellipsometry studies of a polymer molecular layer spread on the water surface. *Langmuir* **1991**, *7*, 3076−3080.

(23) Dussan, E. B.; Chow, R. T.-P. On the ability of drops or bubbles to stick to non-horizontal surfaces of solids. *J. Fluid Mech.* **1983**, *137*, 1−29.

(24) Biot, M. A. General Theory of Three-Dimensional Consolidation. *J. Appl. Phys.* **1941**, *12*, 155−164.

(25) Shanahan, M. E. R.; Carré, A. Spreading and dynamics of liquid drops involving nanometric deformations on soft substrates. *Colloids Surf., A* **2002**, *206*, 115−123.

(26) Park, S. J.; Weon, B. M.; San Lee, J.; Lee, J.; Kim, J.; Je, J. H. Visualization of asymmetric wetting ridges on soft solids with X-ray microscopy. *Nat. Commun.* **2014**, *5*, 4369.

(27) Zhao, M.; Lequeux, F.; Narita, T.; Roché, M.; Limat, L.; Dervaux, J. Growth and relaxation of a ridge on a soft poroelastic substrate. *Soft Matter* **2018**, *14*, 61−72.

(28) Garrido, L.; Mark, J. E.; Ackerman, J. L.; Kinsey, R. A. Studies of self-diffusion of poly(dimethylsiloxane) chains in PDMS model networks by pulsed field gradient NMR. *J. Polym. Sci., Part B: Polym. Phys.* **1988**, *26*, 2367−2377.

(29) Carslaw, H. S.; Jaeger, J. C. *Conduction of Heat in Solids*, 2nd ed.; Clarendon Press: Oxford, 1959.

(30) Bergeron, V.; Langevin, D. Monolayer Spreading of Polydimethylsiloxane Oil on Surfactant Solutions. *Phys. Rev. Lett.* **1996**, *76*, 3152−3155.

DOI: 10.1021/acs.langmuir.8b02128
Langmuir 2018, 34, 12244−12250